

Structural, Immunocytochemical, and MR Imaging Properties of Periventricular Crossroads of Growing Cortical Pathways in Preterm Infants

Miloš Judaš, Marko Radoš, Nataša Jovanov-Milošević, Pero Hrabac, Ranka Štern-Padovan, and Ivica Kostović

BACKGROUND AND PURPOSE: Periventricular white matter (WM) areas are widely recognized as predilection sites for complex cellular damage after ischemia/reperfusion or inflammatory injury of the perinatal cerebrum. We analyzed histochemical and MR imaging properties of fiber architectonics and extracellular matrix (ECM) of periventricular areas to disclose the potential significance of topographically specific WM lesions for the neurodevelopmental outcome.

METHODS: We combined histochemical methods for demonstration of fibers, axonal guidance molecules, and ECM with T1-weighted MR images on postmortem specimens aged 15 to 36 postovulatory weeks (POW) and T2-weighted MR images on in vivo fetuses aged 14 to 26 POW.

RESULTS: The fiber architectonics of the fetal cerebrum display tangential axon strata in frontopolar and occipitopolar regions, whereas the central periventricular region contains crossroads of intersecting callosal (transverse), associative (sagittal), and thalamocortical/corticofugal (radial) fiber bundles. In early preterms, crossroads contain hydrophilic ECM with axonal guidance molecules, and they are easily recognized as hypointensities on T1-weighted MR images or hyperintensities on T2-weighted MR images. After the 28 POW, tangential fetal fiber-architectonic stratification transforms into the corona radiata system; however, the growth of cortical pathways continues in crossroad areas, as indicated by the presence of ECM and their distinct MR imaging signal intensities.

CONCLUSIONS: The correlation of MR imaging with histochemical findings demonstrated the presence of periventricular fiber crossroads rich in ECM and axonal guidance molecules. We propose that, in perinatal WM lesions, periventricular WM crossroads represent a hitherto unrecognized and vulnerable cellular and topographic target in which combined damage of association-commissural and projection fibers may explain the complexity of cognitive, sensory, and motor deficit in survivors of periventricular WM lesions.

Preterm infants are at high risk of developing white matter (WM) injury caused by ischemia/reperfusion

Received November 14, 2004; accepted after revision February 25, 2005.

From the Section for Developmental Neuroscience, Croatian Institute for Brain Research (M.J., M.R., N.J.M., P.H., I.K.), Zagreb, Croatia; and Department of Diagnostic and Interventional Radiology, Clinical Hospital Center Zagreb, School of Medicine, University of Zagreb (M.R., R.Š.P.), Zagreb, Croatia.

This work has been supported by Croatian Ministry of Science and Education (grants 0108115 and 0108118 and the collaborative project grant for Development, Plasticity and Recovery of the Brain after Perinatal Lesion).

Address correspondence to Ivica Kostović, Croatian Institute for Brain Research, School of Medicine, University of Zagreb, Šalata 12, 10000 Zagreb, Croatia.

© American Society of Neuroradiology

and infection/inflammation (1–3). The periventricular leukomalacia (PVL) is a frequent and severe consequence of ischemia/reperfusion injury in preterm infants, who are therefore at high risk of developing motor, cognitive, and behavioral impairments (1, 4–8). In a number of cases, the injury of the WM, originally described as PVL (9), is in fact more widespread and in addition to periventricular WM affects the internal capsule as well as the subcortical and callosal WM (5, 6, 10, 11). Therefore, hypoxic-ischemic WM injuries have been recently reclassified into focal and diffuse lesions (1, 12, 10).

Recent research in pathogenesis and neurodevelopmental outcome of PVL has increasingly and successfully focused on diffuse WM lesions. For example, recent MR imaging studies suggest that diffuse

WM injury with subsequently impaired WM development is extremely common in small premature infants (2, 13) and is commonly manifested as diffuse and excessive high signal intensity (DEHSI) in MR imaging studies by using diffusion-weighted imaging (8, 13, 14, 15), as well as in studies by using conventional MR imaging (16, 17). In addition, recent neuropathologic findings (18) support a growing consensus that both ischemia and infection may lead to activation of microglia and generation of reactive oxygen species and reactive nitrogen species, to which preoligodendrocytes are especially vulnerable (2, 18), and death of these cells likely accounts for the subsequent failure of WM development (1, 2, 19).

In addition to the precise identification of prospective cellular target(s) of hypoxic-ischemic and/or inflammatory lesions, we also need a more precise neuroanatomic and topographic characterization of those lesions, as well as an in-depth knowledge of other developmental processes in the periventricular region during the peak period of the PVL occurrence. At present, there are no detailed neuroanatomic and chemical studies of periventricular fiber systems, the topographic pathology of identified fiber bundles or axon strata and their MR imaging correlates in the periventricular zone of the preterm infant cerebrum; however, a combined neuroanatomic and chemical analysis of identified neural elements is clearly needed because periventricular WM injury in premature infants leads to a complex involvement of different motor, sensory, and associative systems (1, 8, 20), and periventricular WM in the adult brain is known to contain a complex grid of projection (afferent and efferent), commissural (callosal), and major associative ipsilateral cortico-cortical fibers (21–23).

The combined application of *in vivo* MR imaging (7, 14) and detailed neurohistologic analysis of postmortem material (24) is necessary for proper correlation between the exact topography of the WM injury and the neurodevelopmental outcome in surviving preterm infants. The MR imaging opens new possibilities for a detailed analysis and systematization of the cerebral WM in the developing human brain (14) as well as for the follow-up of its structural reorganization after the perinatal lesion (7, 16, 17, 20). Furthermore, to achieve a comprehensive MR imaging diagnosis, we need a precise knowledge of neuroanatomic organization of the preterm infant brain, which changes continuously until birth (25); a careful correlation of MR imaging and histologic findings is required for correctly distinguishing “normal” from abnormal features (13).

In this study, we first combined T1-weighted MR imaging and neurohistochemical techniques on postmortem material to (1) analyze fiber architectonics of the cerebral WM, with focus on periventricular crossroads of major pathways located along the lateral wall of lateral ventricles (ie, at predilection sites of the focal PVL), and (2) analyze the presence of the extracellular matrix (ECM) and the distribution of molecular axonal guidance cues in the periventricular WM during the premyelination stage of development.

It is our hypothesis that intersections of major cortical pathways develop early around ventricles and can be demonstrated on both histologic and MR images due to their characteristic, immature, and growth-related tissue properties. Furthermore, we think that correlated histologic and MR imaging data on strategic periventricular points will help elucidate the role of lesions of fibers and other cellular and extracellular elements in the development of profound but variable pathologic outcome after periventricular WM lesions.

In addition, we analyzed transient patterns of tangential and radial organization of growing fiber systems in the periventricular WM and patterns of their spatial reorganization during the second half of gestation to provide a fiber-architectonic framework for studying the developmental neuropathology and MR imaging changes of the cerebral WM. With this study, we provide an extended and refined spatiotemporal framework of the human fetal WM development to enhance the developmental and neuroanatomic interpretation of findings of modern cellular and molecular studies of cell populations targeted by hypoxic-ischemic and cytotoxic lesions (1–3, 19, 26–28) of the WM in late fetuses and prematurely born neonates.

Finally, we performed fast T2-weighted *in vivo* MR imaging of fetuses aged 14–26 postovulatory weeks (POW) to check whether the changing fiber-architectonic and lamination patterns of the fetal cerebral wall, as visualized on T1-weighted MR images of postmortem specimens, correspond to changing patterns observed in living fetuses.

Materials and Methods

We analyzed postmortem brains of 10 human fetuses (aged 15–26 POW) and 5 prematurely born infants (aged 28–36 POW). Fetal specimens were obtained from medically indicated and/or spontaneous abortions at several clinical departments associated with the University of Zagreb School of Medicine. The fetal age was estimated on the basis of the crown-rump length (CRL, in mm) and pregnancy records and was expressed as POW. In fetuses from both medical and spontaneous abortions, the correlation of maturational parameters (CRL, weight, pregnancy records, and sonographic study at 12 weeks of gestation) revealed no evidence of growth retardation and malformations. The deaths of preterm infants were attributed to respiratory distress syndrome or sudden infant death syndrome. The procedure for the human autopsy material was approved and controlled by the Internal Review Board of the Ethical Committee at the School of Medicine, University of Zagreb. In each case, the parental consent for postmortem examination was obtained.

Whole brains were fixed by immersion in 4% paraformaldehyde in 0.1 mol/L phosphate-buffered saline (PBS), pH 7.4. Before further histologic processing, some specimens were used to obtain the 3D spoiled gradient-echo (3D-GRE) T1-weighted MR images with the high-field 2T MR imaging system (Gyrex Prestige, GEMS/Elscint, Haifa, Israel) and the following parameters: repetition time (TR) 23 ms, echo time (TE) 8.3 ms, number of excitations (NEX) 1, flip angle of 20°, and section thickness of 1.1 mm. The matrix size and the field of view were adjusted to obtain a spatial resolution of at least $0.416 \times 0.416 \text{ mm}^2$. The passive wrist coil with a $9 \times 18 \text{ cm}$ diameter was used following a protocol described elsewhere (24).

Subsequently, brains were cut into tissue blocks, which were

either frozen for acetylcholinesterase (AChE) histochemical visualization of fibers and axon strata or embedded in paraffin for other histochemical methods used in this study. Adjacent Nissl-stained sections were used to delineate the cytoarchitectonic boundaries and cellular compartments of the human fetal telencephalon.

The AChE histochemistry method (29) was used for the direct demonstration of a subset of growing thalamocortical afferents and certain sagittally oriented axon strata, such as the external capsule system. The periodic acid Schiff–Alcian blue (PAS-AB) histochemistry was used to examine the laminar location and relative regional abundance of the ECM at different stages of cortical development (24). To visualize even the thinnest fibers in premyelination and early myelination stages, as well as to reveal an overall fiber-architectonic pattern of the fetal telencephalon, we applied Gallyas silver staining by means of physical development (30) on selected histologic sections adjacent to PAS-AB-stained and Nissl-stained sections.

In the immunocytochemical part of the study, we used the following primary antibodies: (1) the SEMA-3A antibody against the semaphorin3A precursor of human origin (Santa Cruz Biotechnology, Santa Cruz, CA); (2) the EphA3, antibody against the EphA3 receptor protein tyrosine kinases of human origin (Santa Cruz Biotechnology); (3) the MAP-1b, antimicrotubule associated protein 1b (Sigma, St. Louis, MO); (4) the SMI-81, antibody against synaptic protein SNAP-25 (Sternberger Monoclonals, Lutherville, MD); (5) the SMI-312 antibody to phosphorylated neurofilaments (Sternberger Monoclonals); (f) The CS-56, antibody which reacts with chondroitin sulfate (Sigma); and (6) the CD-68, anti-human CD68 cell surface antigen (for identification of microglia, from Serotec, Oxford, UK). We used biotinylated antigoat, antirabbit, and antimouse antibodies from Vectastain ABC kit (Vector Laboratories, Burlingame, CA) according to standard protocols for immunohistochemical staining (31). For the *in vivo* part of the study, we performed fast T2-weighted (HASTE) MR imaging on a 1.5T device (Magnetom Symphony; Siemens, Erlangen, Germany). MR images of normally developing human fetuses aged 13–26 POW were acquired during the medically indicated diagnostic MR imaging pelvic examination in pregnant women displaying vascular pathology in the pelvic region.

Results

Terminology and Parcellation of the Developing Human Cerebral White Matter

Before describing the organization and developmental changes of the fetal WM, we have to define the overall lamination pattern of the fetal telencephalic wall and the terminology used in the Results section. The correlated MR imaging-histologic study (24) demonstrated that the following transient fetal zones are seen on both T1-weighted MR images and histologic sections (from ventricle to pia): (1) the ventricular zone (germinal matrix of high MR imaging signal intensity), (2) the periventricular-subventricular fiber-rich zone (24) of low MR imaging signal intensity, (3) the subventricular-intermediate zone of moderate MR imaging signal intensity, which encompasses the subventricular cellular zone and the fetal WM, (3) the subplate zone of low MR imaging signal intensity, and (4) the cortical plate of high MR imaging signal intensity.

In comparison with the postnatal brain (23), the WM of human fetuses and early premature infants is still poorly developed (compare Figs 2C and 2H with

Figs 2I and 6C) and mostly nonmyelinated. In addition, the thalamocortical radiation does not extend directly to incipient neocortical layers, and the distal part of the corona radiata and the centrum semiovale proper are not yet developed in the midfetal and early preterm cerebrum. Instead, their future positions are occupied by the large and transient subplate zone (32). We found, however, that separate compartments of the human fetal cerebral WM can be meaningfully described by using the segmental parcellation of the adult human telencephalic WM, as classically described by von Monakow a century ago (21): (1) segment I, central WM (including corpus callosum, anterior commissure, fornix, and centrally placed associative fibers); (2) segment II, the region of the corona radiata (Stabkranzregion, ie, the Fuss des Stabkranzes); (3) segment III, the centrum semiovale; (4) segment IV, gyral WM (Markkegel or Markpyramiden); and (5) segment V, cortical white matter (ie, intracortical terminal parts of radial and tangential myelinated fibers).

Development between 15 and 28 POW

Tangential Axon Strata and Laminar Organization of the Fetal WM. During the midfetal period (ie, between 15 and 28 POW and before the onset of gyrification), the tangential stratification of major fiber systems is the dominant fiber-architectonic feature of frontal, dorsal-midlateral, temporal, and occipital parts of the cerebrum (Figs 1–4), with the exception of its midlaterobasal and medial limbic parts. Tangentially arranged fiber systems occupy the periventricular-subventricular region and the intermediate zone, and separate systems can be delineated at different depths: (1) periventricular-subventricular fiber systems are located adjacent to the ventricular surface (Figs 1, 4B, -D); (2) thalamocortical fibers are tangentially stratified within the intermediate zone (Figs 1, 2B, -D, -F, 4); and (3) the outermost part of the intermediate zone is occupied by the external capsule system, which also marks the border of the WM toward the subplate zone (Figs 1, 2B, -D–G, 4). The subplate zone displays a loose fibrillar network (Fig 1). On the other hand, the tangential position of cortical efferent projection systems cannot be precisely determined, because there is no reliable method for their selective visualization; these fiber systems usually remain unlabeled in differently stained sections, but at least some of them seem to display SNAP-25-immunoreactivity (Fig 4B).

The corpus callosum is located closest to the ventricular system. Its fibers do not stain by AChE-histochemistry (Fig 2B, -D, -F, -G). They represent a pale area in Nissl-stained sections (Fig 2A) and remain unstained in Gallyas preparations (Figs 1, 5A). The fibers of the callosal system represent an important component of the periventricular-subventricular fiber-rich zone (*asterisks* in Fig 2C, -H; *pale areas* in Fig 2B, -F, -G). The periventricular-subventricular fibrous zone is clearly delineated on T1-weighted MR images due to its very low MR imaging signal inten-

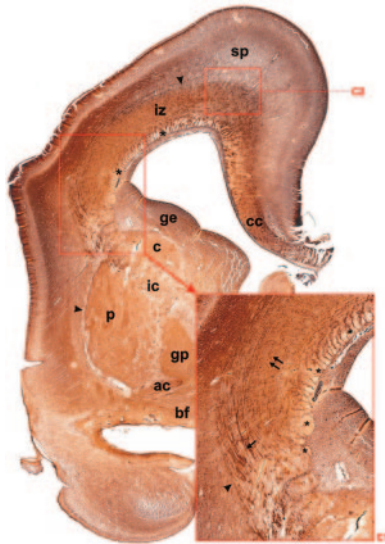


Fig 1. The coronal section through the telencephalon of 18-week-old human fetus, Gallyas silver staining. Note that fiber bundles and their crossings are located in the fetal “white matter”—ie, in periventricular region (C1, C2, and asterisks)—and the intermediate zone (iz), whereas the subplate zone (sp) is characterized by a loose (“isotropic”) argirophilic network of fibers. The fetal “white matter” consists of tangentially stratified fiber bundles such as external capsule (*arrowheads*), corpus callosum radiation (cc), thalamocortical projection fibers (*arrow*), and the deep system (*double arrows*; see insert C1). In addition, a prominent periventricular system of unstained and transversely or obliquely cut fiber bundles (*row of asterisks*) is situated in the subventricular zone. Abbreviations for this and subsequent figures: a = amygdala; ac = anterior commissure; bf = basal forebrain; c = caudate nucleus; C1–C6 = crossroad areas; cc = corpus callosum; ge = ganglionic eminence; gp = globus pallidus; ic = internal capsule; iz = intermediate zone; p = putamen; sp = subplate zone; th = thalamus.

sity (Fig 2C, *asterisks*; Fig 2H). The most massive part of the corpus callosum is at the level of the interventricular foramen and rostral part of the anterior horn of the lateral ventricle (Figs 2A, -B). The callosal fiber system is still well developed in the occipital lobe, but it becomes very thin in the depth of the calcarine fissure (Figs 2G, -H). The transition of the main trunk of the corpus callosum into the more stratified periventricular-subventricular zone occurs at the dorsal angle of the lateral ventricle (Figs 1, 2B, -F, 4B, -D).

A prominent component of periventricular-subventricular fiber systems is derived from the corpus callosum, which is the thickest central bundle. Another prominent component of the periventricular-subventricular fiber-rich zone is a row of relatively thick and predominantly rostrocaudally oriented fiber bundles, which remain unstained in Gallyas sections (Fig 1, *asterisks*) or CS-56-stained sections (Fig 4D, *asterisks*), but do display SNAP-25-immunoreactivity (Fig 4B). These peculiar subventricular fiber bundles are more prominent at midlateral levels and diminish in size in the dorsomedial part of the cerebral wall, where they become intermingled with callosal fibers (Fig 4B); basolaterally they merge with the fountainhead of the internal capsule (*asterisks* in Fig 1, inset).

The intermediate zone represents the most exten-

sive laminar compartment of the fetal WM and can be clearly recognized in T1-weighted MR images because of its significantly increased MR imaging signal intensity (Figs 2C, -H). The thalamocortical system of fibers fans out through the fountainhead of the internal capsule (Figs 1, 2B, -F, 4A, -C) and in a number of arching bundles spreads throughout the width of the intermediate zone, up to its outer border marked by the external capsule system (Figs 1, 2B, -D, -F, 4A, -C). Whereas the Gallyas staining visualizes only major fiber bundles of the internal capsule and proximal (peduncular) portion of the thalamocortical radiation (Fig 1), the AChE-histochemistry provides a detailed and extensive visualization of at least some subpopulations of thalamocortical axons (29).

In the frontal lobe, these fibers occupy a zone wedged between 2 sagittal stripes, which display much stronger AChE-reactivity (Fig 2B, -D) and correspond to von Monakow’s internal and external sagittal stratum (21). The inner stripe is adjacent to AChE-negative callosal periventricular fibers and the subventricular zone, and the outer stripe represents an external stratum, which merges with the external capsule. Both AChE-reactive stripes are also present in the occipital lobe (Fig 2D, -G), where they are situated more closely to each other and display even stronger AChE-reactivity. The ECM of the intermediate zone can be selectively visualized by PAS-AB histochemistry (pink in Fig 2E), which also displays CS-56-immunoreactivity, especially in the outer part of the intermediate zone (Fig 4D). The immunocytochemical marker SMI-312 enables the visualization of some subpopulations of fibers within the intermediate zone, especially in its outer and midlateral portion (Fig 4C).

The external capsule system emanating from the basal forebrain represents the most superficial tangential stratum of the fetal WM, and marks its border toward the subplate zone (*arrowheads* in Figs 1, 3, 4). On T1-weighted MR images, the capsula externa is visible basolaterally along the putamen (Fig 2C, *black arrowhead*), but in the dorsal part of the cerebral wall it cannot be directly visualized. However, its position is clearly indicated by the sudden decrease in the MR imaging signal intensity at the transition from the intermediate zone to the subplate zone (Fig 2C, -H, *arrowheads*).

The analysis of *in vivo* acquired HASTE sequence images revealed the same typical fetal lamination pattern of the cerebral wall (Fig 3). In comparison to T1-weighted MR images of postmortem specimens, MR imaging signal intensities on *in vivo* T2-weighted images (Fig 3A) display the reversed pattern: the hypointensity of the ventricular zone, the moderate intensity of the subventricular zone, the hyperintensity of the intermediate zone (Fig 3A, -B), and the hypointensity of the cortical plate (Fig 3A). Note that at 14 POW (Fig 3A) the subplate zone is still in the subplate formation stage (32) and therefore cannot be clearly visualized on MR images. However, at 26 POW, the subplate zone is clearly recognizable as a

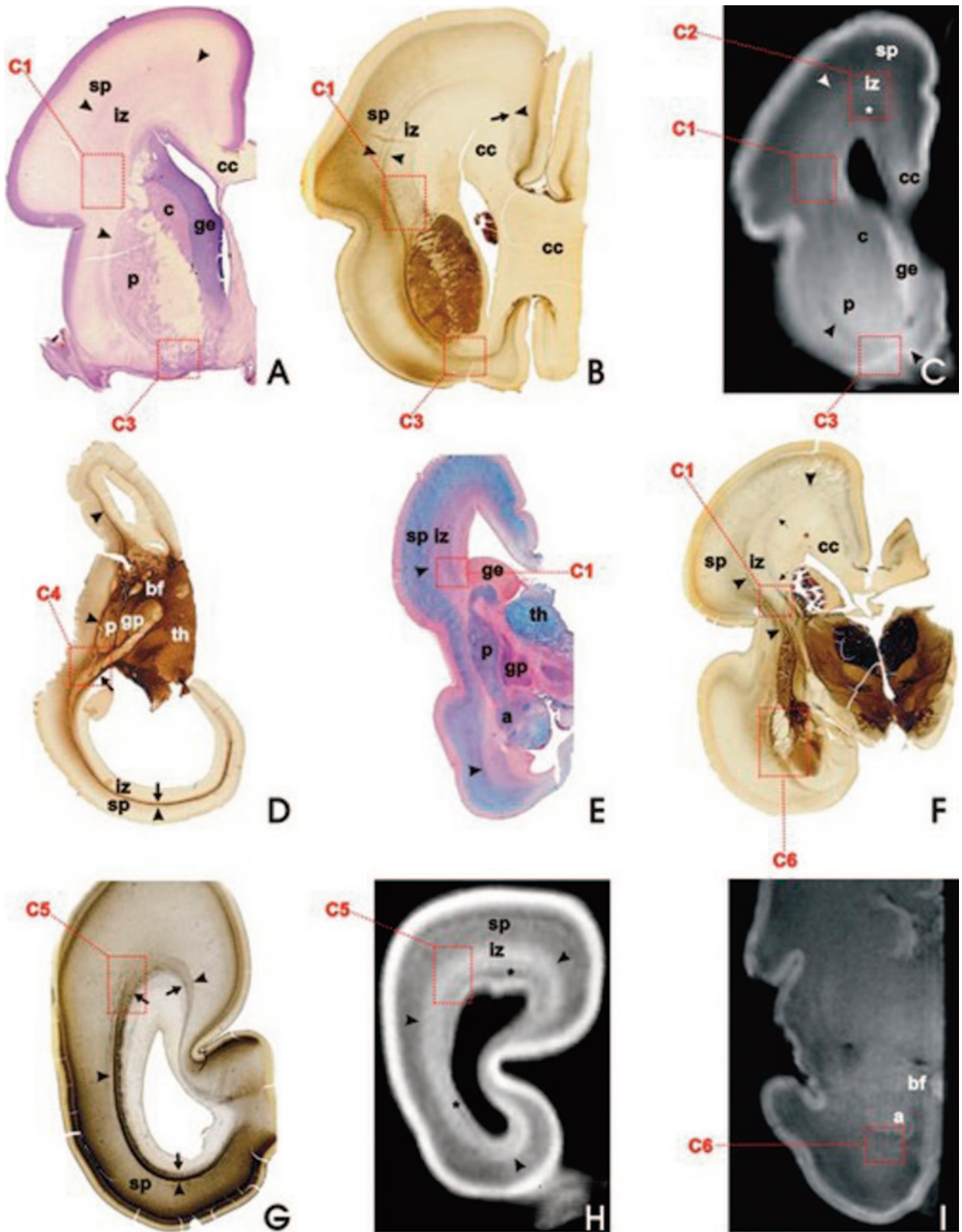
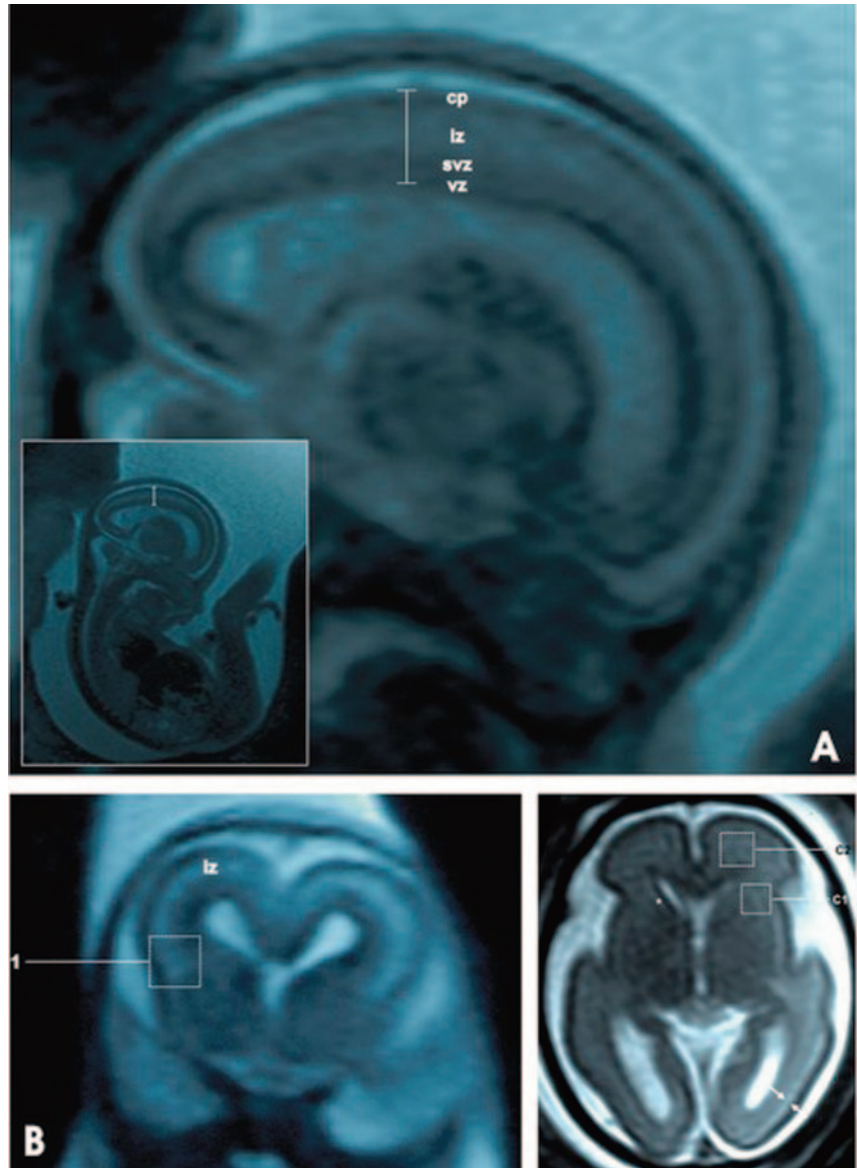


FIG 2. During the fetal lamination stage (16–24 weeks of gestation), the basic fiber-architectonic pattern is characterized by predominantly tangential organization (axon strata) and prominent crossroads (C1–C6, *dashed squares*) of projection, association, and commissural fibers, as revealed on coronal (A–C and E–I) and horizontal (D) sections; Nissl-stained (A), AChE-stained (B, D, F, G), PAS-AB-stained (E), and T1-weighted MR imaging sections (C, H, I); in fetuses aged 16 weeks (D), 18 weeks (G, H), 19 weeks (A, E), 21 weeks (B, C), and 24 weeks (F). After 28 weeks of gestation, MR imaging signal intensity changes with consequent blurring of laminar pattern, as revealed by T1-weighted MR coronal section through the cerebrum of 30-week-old fetus (I). Asterisks in C and H mark the periventricular-subventricular fiber system.

FIG 3. In vivo acquired fast T2-weighted MR images (HASTE sequence) in 14 POW (A and B) and 26 POW (C) fetuses reveal the same typical fetal lamination pattern of the cerebral wall as T1-weighted MR images of postmortem specimens of equivalent developmental ages. In panel A (and its inset), the vertical bar denotes the thickness (approximately 5 mm) of the entire telencephalic wall. Inhomogeneous, poorly delineated, spotlike area (dotted rectangle marked as C1 on panels B and C) of higher MR imaging signal intensity corresponds to the main crossroad area. Larger, rectangularly-marked spotlike area above corresponds to C2 crossroad area. In panel C, asterisk marks the fibrillar periventricular-subventricular zone, while the subplate zone is situated between 2 arrows. Other abbreviations as in Fig 1. For further details, see text.



hyperintense zone on in vivo T2-weighted MR images (Fig 3C).

Periventricular Crossroad Areas. In the fetal WM, there are at least 6 periventricular areas in which major cortical projection, association, and commissural systems form a complex grid of intersecting fibers. On the basis of their topographic position, fiber composition, and intersection, we designate them numerically as periventricular crossroad areas C1–C6 (Figs 1, 2), due to the lack of generally accepted terminology. These periventricular crossroad areas are characterized by an abundant and hydrophilic ECM and low signal intensity on T1-weighted MR images and can be best visualized in coronal sections through the fetal telencephalon by means of different staining techniques. The first 3 crossroad areas (C1–C3) are located in the frontal lobe, the fourth (C4) is in the parietal region, the fifth (C5) is in the occipital lobe, and the sixth (C6) is in the temporal lobe.

The Main Frontal Crossroad Area C1. The main (and the largest) crossroad area C1 is located lateral to the lateral angle of the lateral ventricle, at coronal levels through the septum and the interventricular foramen, where fibers of the anterior limb of the internal capsule emanate between the caudate nucleus and the putamen (Figs 1, 2A–C, -E, -F, 4). The position of the C1 is also recognizable on in vivo T2-weighted MR images as an area of higher MR imaging signal intensity (Fig 3B, -C). At rostral (septal) levels, the immature anterior horn is pear-shaped (Fig 1) and has one lateral and one dorsal angle (the mature anterior horn has a single angle, in which the corpus callosum arches over the head of the caudate nucleus). The C1 is cashew-shaped (Figs 1, 5), with its concave margin capping the fountainhead of the internal capsule (ie, the peduncular part of the prospective corona radiata) and the dorsolateral edge of the caudate nucleus and the ganglionic eminence. Its lateral margin touches the dorsal edge of the putamen,

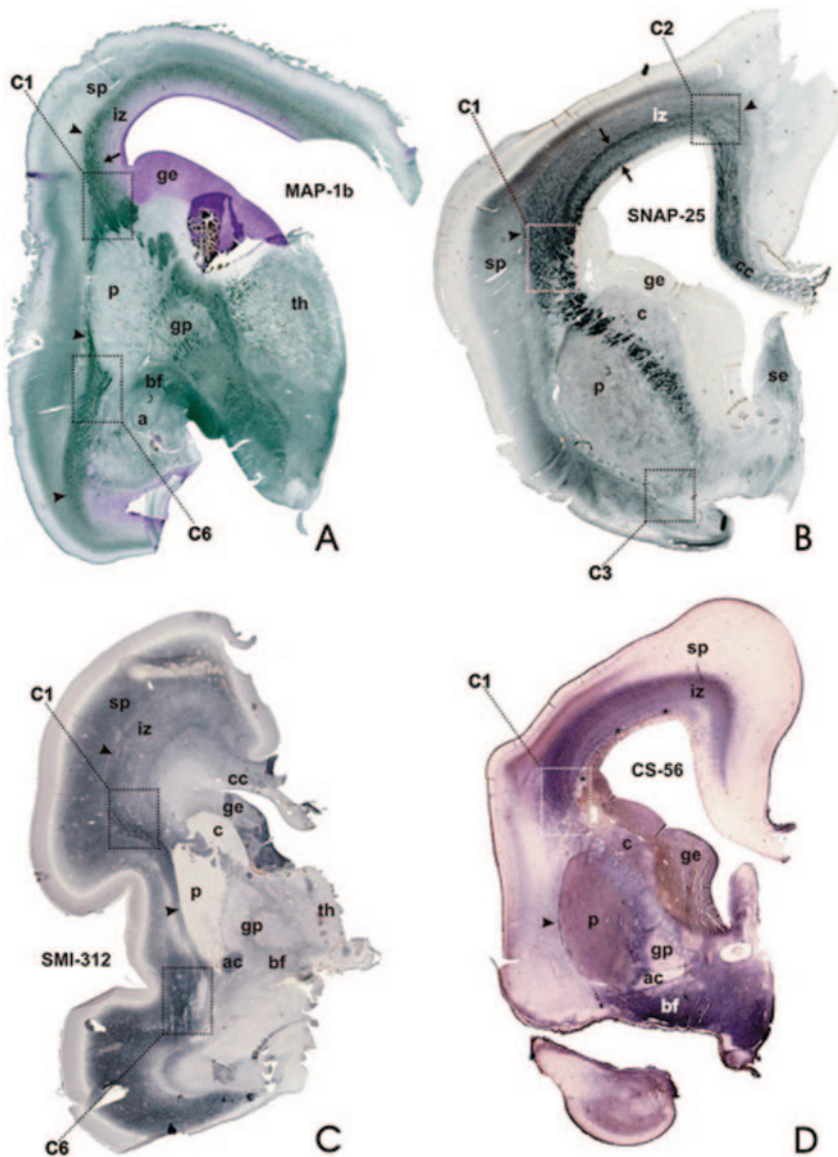


FIG 4. During the stage of typical fetal lamination, various immunocytochemical markers selectively label discrete contingents of fibers within the stratified periventricular fetal WM (iz): MAP-1b (A, 18-week-old fetus) and SMI-312 (C, 20-week-old fetus) label the cytoskeletal components of many growing axons, whereas the prominent periventricular system of fiber bundles is stained by SNAP-25 antibody (B, 18-week-old fetus, *arrows*). These markers are also visualizing periventricular fiber crossroad areas (C1, C2, C3, C6). Note that CS-56 antibody (D, 18-week-old fetus) labels the extracellular matrix, but is not expressed within the periventricular fiber system (*asterisks*). *Arrowheads* denote the capsula externa system, which marks the border between the fetal WM (iz) and the subplate zone (sp), which is part of the neocortical anlage.

while its medial margin extends along the lateral angle of the lateral ventricle and the lower part of the callosal radiation. The outer, convex margin of the C1 runs along the interface between the external capsule and the subplate zone (Figs 1, 4). As revealed by PAS-AB histochemistry (Fig 2E) and chondroitin sulfate CS-56 immunocytochemistry (Fig 4D), the C1 contains an abundant ECM.

The C1 is also recognizable on T1-weighted MR images because of its reduced MR imaging signal intensity and its patchy appearance (Figs 2C, 5C). The Gallyas impregnation (Fig 1) and the AChE-histochemistry (Fig 2B, -F) reveal that the C1 contains thick bundles that emanate from the internal capsule, contain thalamocortical fibers, and arch dorsally through the outer third of the intermediate zone (ie, the fetal WM). These arching fibers laterally intersect with fibers emanating from the external capsule, whereas medially they intersect with the most

superficial fibers of the callosal system in the periventricular-subventricular fibrous zone (Fig 1, inset).

The bundles of SNAP-25-immunoreactive fibers of the subventricular zone become thicker as they approach and enter the C1 (Figs 1, 4B). In addition, the C1 contains many MAP-1b-immunoreactive (Fig 4A) and SMI-312-immunoreactive (Fig 4C) growing axons. As revealed on Nissl-stained sections (Fig 2A), the grid of intersecting fibers in the C1 contains numerous cell bodies which probably represent migratory neurons and immature glial cells (at least as judged on the basis of their shapes and sizes of their nuclei). Finally, CD-68 immunohistochemistry demonstrated the presence of microglia in the C1 (Fig 6C).

The Frontal Crossroad Area C2. The second frontal crossroad area C2 is located above the dorsal angle of the immature anterior horn of the lateral ventricle, as seen on histologic sections (Figs 1, 4B, 5A), T1-weighted MR images (Figs 2C, 5C), and T2-weighted

FIG 5. SEMA3A immunoreactivity (A, 20-week-old fetus) is restricted to median and paramedian parts of the callosal radiation, where it is located in both cell bodies and the extracellular matrix in the ventral part of the corpus callosum (*asterisk*), and in the fornix system (*arrow*). The SEMA3A immunoreactivity is also located in the roof of the anterior horn of the lateral ventricle, corresponding to the frontal crossroad area C2 (dashed square in B, 20-week-old fetus). In addition, the expression of CD68 marker for microglia (C, 18-week-old fetus) is most prominent in the frontal crossroad area C2 (*dark dots*).

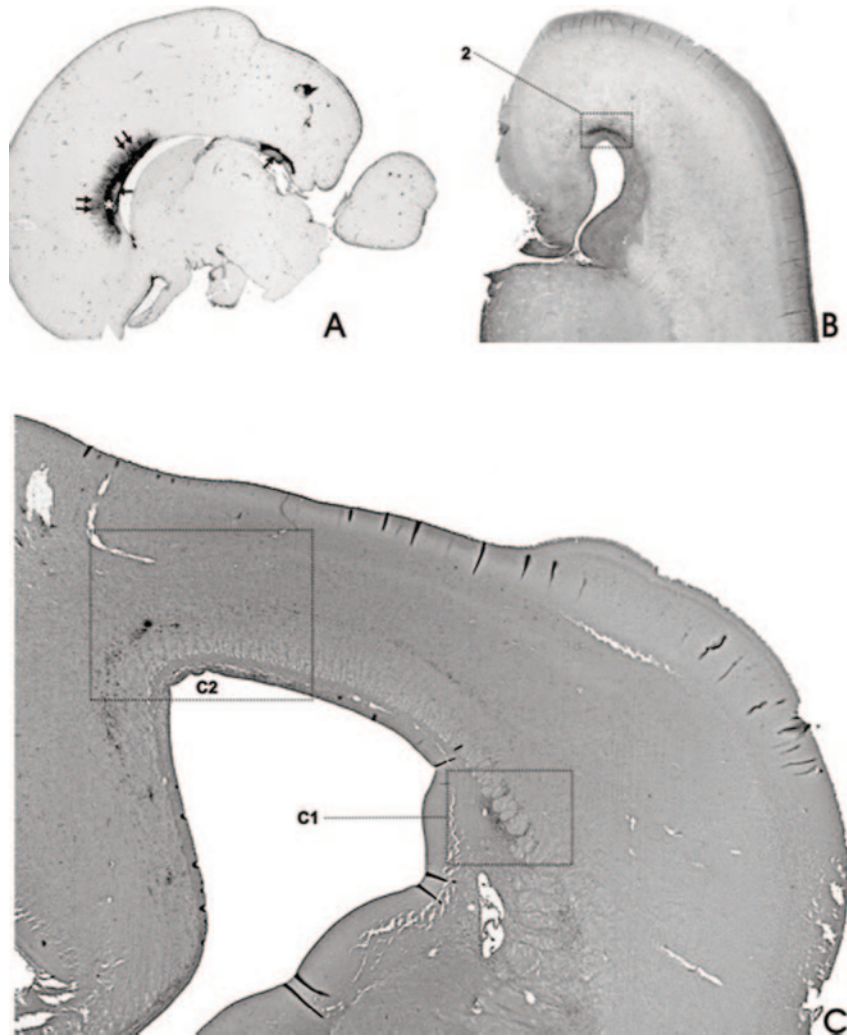
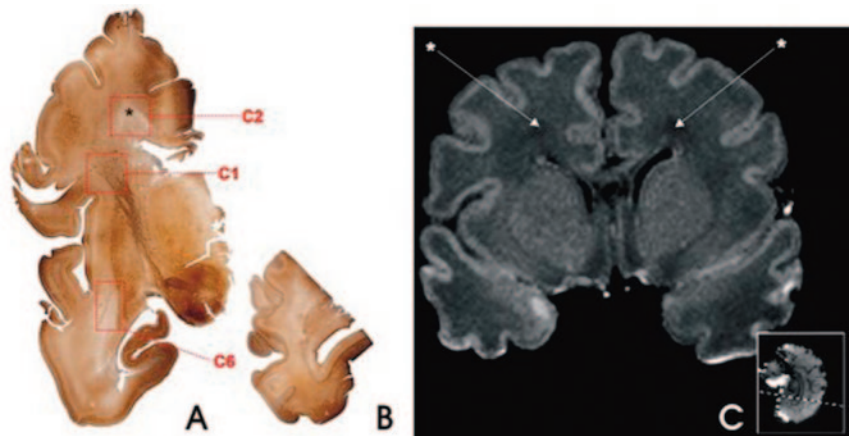


FIG 6. The outlines of the corona radiata appear after 28 weeks of gestation. Gallyas staining (A and B, 33-week-old pre-term neonate) and MR image (C, 36-week-old neonate). The peduncular part of the corona radiata corresponds to the major frontal crossroad area (C1 in A); however, the centrum semiovale (*asterisk* in A) still displays signs of immaturity and corresponds to the crossroad area C2. This is manifested as pale (ie, poorly myelinated) area in Gallyas-stained sections (C2 in A) and as patches of decreased MR imaging signal intensity in T1-weighted MR images (C, asterisks). Note that tangential stratification of sagittally oriented fibers is still well preserved in the occipital white matter (B) and that temporal crossroad area (C6 in A) is still poorly myelinated in the pre-term neonate.



in vivo MR images (Fig 3C), especially in fetuses older than 20 POW. In the C2, callosal fibers closely follow the curvature of the periventricular-subventricular zone and intermingle with thalamocortical and other projection pathways of the intermediate zone. Certain axon guidance molecules display an interesting distribution within the corpus callosum and the C2. Namely, SEMA-3A-immunoreactivity

(Fig 6A) is restricted to median and paramedian parts of the callosal radiation, while EphA3-immunoreactivity remains restricted to the C2 (Fig 6B). In addition, the C2 is particularly rich in CD-68-immunoreactive microglial cells (Fig 6C).

The Frontal Crossroad Area C3. The third crossroad area C3 is located ventral to the caudate-putamen at the level of the callosal knee, and extends rostrally in

a close apposition to the bottom of the anterior horn of the lateral ventricle (Figs 2A–C, 4B). It contains AChE-reactive fibers originating from subcallosal bundles and the external capsule (Fig 2B) as well as AChE-negative fiber bundles originating from the corpus callosum, the anterior commissure and the internal capsule. On T1-weighted MR images (Fig 2C), the C3 is recognized as an area of the reduced MR imaging signal intensity, wedged between the ventral border of the caudate-putamen and the ventral extension of the ventricular zone.

The Parietal Crossroad Area C4. The parietal crossroad area C4 is located at the exit of the retroventricular portion of the posterior limb of the internal capsule (Fig 2D). On horizontal sections, the C4 has a triangle shape with the base corresponding to the exit of the internal capsule and the tip formed by 2 convergent and sagittally oriented AChE-reactive bundles (Fig 2D). It contains fibers of the developing primary visual pathway (ie, geniculocortical projection) as well as AChE-reactive fibers from the pulvinar, AChE-negative callosal fibers, and most probably other, sagittally oriented, associative corticocortical fibers.

The Occipital Crossroad Area C5. The occipital crossroad area C5 is located dorsolateral to the posterior horn of the lateral ventricle, close to the parietooccipital junction (Fig 2G, -H). In the C5, AChE-reactive fibers originating from pulvinar and the basal forebrain intermingle in the external capsule system and mix with AChE-negative fibers of the callosal radiation (Fig 2G).

The Temporal Crossroad Area C6. The temporal crossroad area C6 is located anterolateral to the tip of the inferior horn of the lateral ventricle (Figs 2F, -I, 4A, -C, 5A). A massive contingent of AChE-reactive fibers emanating from the basal forebrain fans out through the periamygdaloid area (Fig 2F). These AChE-reactive bundles of fibers are intermingled with AChE-negative bundles belonging to the inferior radiation of the internal capsule, the posterior radiation of the anterior commissure, and the amygdalofugal system (Fig 2F). The position of these fibers is also visible on T1-weighted MR images (Fig 2I) because of the decrease and inhomogeneity of MR imaging signal intensity along the basal and basolateral margin of the amygdala. In addition, the C6 contains MAP-1b-immunoreactive (Fig 4A) and SMI-312-immunoreactive (Fig 4C) fibers. As indicated by PAS-AB histochemistry (Fig 2E), the ECM of the C6 is also enriched with acid-sulfated glycoconjugates.

Development after 28 POW

After 28 POW, the most conspicuous change (clearly visible on both histologic sections and T1-weighted MR images) in the organization of the cerebral wall is the reorganization and gradual disappearance of the fetal lamination pattern, caused by 2 concurrent processes: gradual rearrangement of major fiber systems and gradual resolution of the fetal subplate zone. Thalamocortical projection fibers now

extend radially to the cortical plate, thus forming the core of the incipient centrum semiovale and the corona radiata (Fig 5); however, the remnant of significantly reduced subplate zone is still interposed between the corona radiata and the cortical plate in the gyral WM. The Gallyas staining shows that the extent of the fetal WM is significantly increased, which indicates an early myelination in the main crossroad area (Figs 5A, -B).

The methods applied in this study did not allow the identification of short associative fiber bundles. Long associative bundles, however, are better developed in the late fetus, and their appearance at some places is closely related to the onset of gyrification. For example, on T1-weighted MR images (Fig 5C) the cingulum bundle is visible within the cingulate gyrus as a circumscribed round area of the decreased MR imaging signal intensity. The central part of the C2 (Fig 5C, *asterisks*) also displays the low MR imaging signal intensity on T1-weighted MR images and is still poorly myelinated (Fig 5A, *asterisk*). This area probably corresponds to the fronto-occipital bundle (fasciculus longitudinalis medialis). It should be noted that subventricular fiber bundles, so prominent during the midfetal period, are no longer visible in the late fetus.

The main segments of the cerebral WM and the corona radiata, as described by von Monakow (21), are now recognizable for the first time in Gallyas-stained coronal sections (Fig 5A): (1) the central WM (segment I), (2) the peduncular part of the corona radiata (segment II), (3) the centrum semiovale (segment III), and (4) the gyral white matter (segment IV). However, the fifth, most distal segment (ie, the intracortical myelinated fiber network) still cannot be visualized. On the basis of its topographical location and gridlike arrangement of fibers, the main frontal crossroad area C1 obviously corresponds to the peduncular part of the corona radiata, ie, the segment II (Fig 5A).

The periventricular crossroad areas still retain their basic topographic relationships, histochemical properties, and MR imaging features on T1-weighted images. However, findings of PAS-AB histochemistry and chondroitin sulfate immunocytochemistry clearly suggest that the amount of the ECM is decreased in comparison to the midfetal period. The C1 displays an increased number of myelinated fibers on Gallyas-stained sections (Fig 5A). As the shape of the lateral ventricle has changed, the C2 has shifted laterally and located adjacent to the C1. Namely, the maturing anterior horn has narrowed, while a single, lateral angle has replaced 2 angles characteristic for the fetal stage. Gallyas preparations revealed that the region encompassing the C2 and the dorsolateral part of the C1 is still poorly myelinated (Fig 5A, *asterisk*), probably because it contains late-developing associative fronto-occipital fiber systems.

The ventral frontal crossroad area C3 contained a grid of AChE-reactive fibers from the external capsule and AChE-negative fibers from the corpus callosum and still displayed a decreased MR imaging

signal intensity on T1-weighted MR images (Fig 5C). The thickness of fiber bundles within the temporal crossroad area C6 has increased, but the caudal part of the C6 continues into the sagittal strata of fibers along the lateral wall of the temporal horn of the lateral ventricle (Fig 5A). The occipital crossroad area C5 contained intersections of myelinated fibers of the external capsule and less myelinated fibers from the internal capsule radiation. In comparison to fiber systems in other crossroad areas, the occipital system retained clearly stratified arrangement of fibers (Fig 5B).

Discussion

In the present study, we described major periventricular fiber systems, their crossroads, immunocytochemical properties, and developmental transformation in the cerebrum of the preterm infant, thus confirming and extending previous histologic and MR imaging findings (14, 17, 21, 22, 24, 29, 33–35). In addition, we demonstrated that MR imaging findings obtained on postmortem specimens (T1-weighted images) closely correspond to MR imaging findings obtained in vivo (T2-weighted images). Thus, our findings could be usefully applied in diagnostic neuroimaging of normal and disturbed development of the human fetal and perinatal brain.

With respect to fiber architectonics of the human fetal telencephalon, we presented 2 main findings: (1) in preterm infants, we delineated the period in which the predominant orientation of major fiber systems changes from tangential into the radial; and (2) in the periventricular WM, we demonstrated the existence of characteristic crossroad areas; these areas of intersecting growing fibers display an increased amount of the ECM and axon guidance molecules, and transient low (on T1-weighted images) or high (on T2-weighted images) MR imaging signal intensity.

Development of Centrum Semiovale Proper and the Distal Corona Radiata

Previous histochemical and MR imaging studies (25, 29, 32, 35, 36) demonstrated that, in the cerebrum of human fetuses and very preterm infants, the main fiber systems are predominantly stratified in tangential axon strata. The initial tangential stratification of major fiber systems corresponds to the overall cytoarchitectonic stratification of the fetal cerebral wall, which consists of tangentially arranged architectonic zones (24, 25, 37). The typical fetal lamination pattern was successfully visualized in recent MR imaging studies, too (16, 17, 24, 33, 34, 38, 39). In frontal and occipital lobes of the fetal cerebrum, tangential axon strata represent developmental primordia of sagittal strata in the adult brain, as described in both classical (21) and modern studies (23). It should be noted, however, that, already at early developmental stages, midlateral and basolateral parts of the cerebral wall are characterized by radial extension of thalamocortical fibers toward the neocortical anlage

(29) and thus represent an exception to the general principle of tangential stratification.

A major finding of our study is that the transformation of fiber-architectonic pattern from predominantly tangential in fetuses to predominantly radial in preterm infants occurs concomitantly with several other events: (1) the development of distal portions of the corona radiata and the centrum semiovale proper, (2) the dissolution of the transient fetal subplate zone, (3) the relocation of cortical afferents from the subplate zone into the cortical plate, and (4) the onset of gyrification (32, 40). Thus, the transformation of fiber architecture occurs during the well-delineated developmental window (28–34 POW), which corresponds to the important phase in development of cortical connectivity (24, 32, 40) and can be traced in both histologic sections and MR images. Our findings enable a more precise delineation of that important and vulnerable period, which was already noted in other developmental neuroimaging studies (14, 16, 33, 34, 40).

Which fiber system(s) contribute most prominently to the rapid development of the corona radiata from 28 to 34 POW? At present, there are no clear answers to that question. There is, however, little doubt that a significant contributor to the expansion of the corona radiata is the enlargement of the thalamocortical system, which relocates from the subplate zone into the cortical plate from 24 to 26 POW (24, 32, 40). In addition, callosal (commissural) and ipsilateral associative fiber systems intermingle in the subplate zone between 28 and 33 POW (32) and gradually relocate into the cortical plate, thus contributing to the formation of distal portions of the corona radiata within the gyral WM—ie, the Markkegel of von Monakow (21).

Another contingent of long ipsilateral corticocortical fibers, which contribute to the transformation of fiber architectonics in both distal and central (periventricular) WM regions is represented by prominent SNAP-25-immunoreactive bundles of axons which we described in the subventricular zone, just above and lateral to the ganglionic eminence. These peculiar subventricular fiber bundles are transiently present in fetuses, before the onset of cortical gyrification, but disappear in preterm infants (ie, concomitantly with the development of corona radiata and reshaping of the anterior horn of the lateral ventricle). It should be pointed out that these transient fiber bundles are present during the period of neuronal migration and thus may also represent the substrate for tangential axonophyllic migration of cortical interneurons on their long and tortuous journey from the medial ganglionic eminence through the subventricular zone to the cortical plate (50, 51). A special fibrous layer (inner fiber layer), supposedly nonexistent in the rodent brain, was recently described in the subventricular zone of fetal rhesus monkey cerebrum (40). We were able to delineate similar periventricular-subventricular fiber systems in both histologic and MR imaging sections.

The finding of this “new” fiber system in the periventricular region should be taken into consider-

ation when interpreting the consequences of the most common WM lesion, the PVL (1, 9). Previous studies mostly considered anatomic substrate for motor deficit in the cerebral palsy after PVL lesions (1, 20). It was proposed that descending corticospinal fibers are frequently affected because in the internal capsule they are situated more closely to the periventricular locus of necrosis (1, 20). Our study indicates that other periventricular fiber systems may be damaged within the developmental window crucial for tangential-to-radial transformation of cerebral fiber architectonic.

Development of Periventricular Crossroad Areas

The major finding of our study is that periventricular crossroad areas develop early and already in the midfetal period contain a complex grid of intersecting projection, association and commissural fibers. Furthermore, that axonal grid is embedded in an abundant and hydrophilic ECM rich in axonal guidance and growth-promoting molecules. This is an important fiber-architectonic feature of the developing WM, which was not described in previous studies because of the lack of use of appropriate staining methods. Developmental neuroimaging studies also failed to describe periventricular crossroad areas, probably because they were focused on laminar development (24, 33, 38) and possible migratory phenomena (17, 41) in the periventricular region. It is quite probable that some localized and well-delineated areas of low MR imaging signal intensity described in the periventricular region of preterm infants (15) in fact correspond to periventricular crossroad areas in the otherwise normal brain (38), as described in our study.

Which populations of growing axons intersect in periventricular crossroad areas? Our findings indicate that they include thalamocortical axons, ipsilateral and callosal cortico-cortical axons, chemically identified axons such as afferent projection from the cholinergic basal forebrain, and probably subsets of efferent cortical projection fibers. Moreover, thalamocortical projections are not just those destined for prospective sensory cortical areas, but also projections from the mediodorsal nucleus and the pulvinar, which are destined for prefrontal, anterior cingulate, and parietotemporal association areas involved in cognitive functions, such as working memory and attention. Therefore, we predict that the neurodevelopmental outcome after hypoxic-ischemic and/or inflammatory periventricular lesions, which damage crossroad areas, almost by default will be characterized by various combinations of motor, sensory, behavioral, and cognitive deficits.

This prediction is in accordance with observations of complex neurodevelopmental and cognitive deficits after periventricular lesions in preterm infants (2, 3, 27, 42). Moreover, the concept of periventricular fiber crossroads explains both the topographic and developmental-cellular basis of the vulnerability of the periventricular WM. The developmental signifi-

cance of periventricular crossroads emerges from the fact that fibers interact at crossroads and use different molecular guidance cues and different growth substrates. Putative molecular interactions within the periventricular crossroad areas may be crucial for subsequent growth and spatial arrangement of fibers, after they leave the crossroads. For example, growing axons that enter crossroads may be rerouted upon the contact with various attractive or repellent axon guidance cues (43, 44) or macromolecular components of the ECM (44–46).

Our findings indicate that periventricular crossroad areas contain both the abundant ECM and several major types of axon guidance cues defined in previous experimental studies, such as ephrins and semaphorins. Therefore, it is important to realize that ischemic-hypoxic and/or inflammatory lesions of crossroad areas would not only disrupt growing axons and premyelinating oligodendrocytes, but also cause a transient or permanent disturbance in functioning of signaling cascades involved in the maintenance and proper navigation of growing axons. With respect to that, the PVL or the hemorrhage may have a number of deleterious effects, ranging from bulk destruction of the ECM, axon guidance cues and cells that produce these molecules, to more subtle (but potentially equally damaging) changes in relative quantities and proper 3D distribution of axon guidance cues.

Massive lesions of periventricular tissue, as observed in the PVL and PVH, certainly damage crossroads, which are situated exactly at predilection sites for those lesions. So, the question is not whether such lesions damage periventricular crossroad areas, but whether we understand the relative importance of their cellular components (fibers, the ECM, guidance cues) for the development of cortical pathways. We propose that the disruption of the 3D architecture of the ECM and axon guidance cues embedded in it should be regarded as an additional potential cause of unfavorable neurodevelopmental outcome after hypoxic-ischemic or inflammatory lesions of periventricular crossroad areas. The precise nature of cells producing ECM components and axon guidance cues within the crossroad areas is still unknown, but recent studies demonstrated that both neurons and glia may undergo apoptosis after the hypoxic-ischemic lesion (28). Therefore, on the basis of this and previous developmental studies in human cerebrum (24, 25, 28, 29, 32, 34, 35, 40, 46–49), we designed an overview diagram of complex relationships and possible cellular targets in the periventricular region (Fig 7).

Obviously, the injury of premyelinating oligodendrocytes can easily shift the balance of glial-neuronal interactions and disturb the myelogenesis, thus compounding the effects of axonal injury and interfering with proper myelination and the establishment of proper neuronal connections (26). In fact, recent experimental studies on effects of hypoxia-hypovolemia as well as observations in human infants (1, 12, 19) have suggested that hypoxic and cytotoxic injury of oligodendroglia may represent a key pathogenetic mechanism of the developmental WM lesion. That

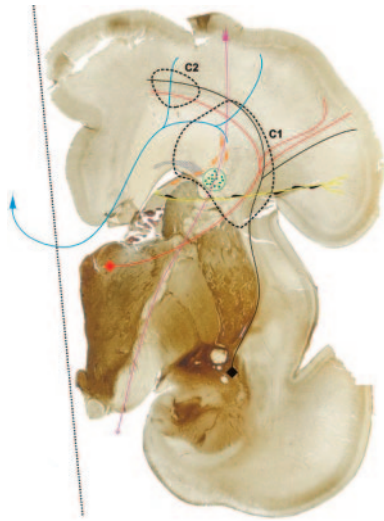


FIG 7. Summary diagram, superposed on AChE-stained coronal section through a telencephalon of 28-week-old human fetus constructed on the basis of our data and evidence from current literature. Thick black dashed lines delineate the first (C1) and second (C2) frontal crossroad area. The honeycomb pattern area denotes the deep periventricular system of fiber bundles; and circle with green dots developing fronto-occipital system, both containing SNAP-25 immunoreactive fibers. Colored lines denote systems of projection, association and commissural fibers passing through the crossroads (with triangles or quadrangles depicting cell bodies of origin), as follows: black = basal forebrain afferents; red = thalamocortical afferents; blue = callosal fibers; violet = corticofugal efferents. Note that both radially migrating neurons (black profiles along the yellow radial glial fiber) and tangentially migrating neurons (orange profiles) pass through the major crossroad (C1) area, which is located at the main predilection site of hypoxic-ischemic lesion in preterm infants.

concept by no means contradicts our emphasis on molecular composition and fiber arrangements of periventricular crossroad areas—namely, vulnerable oligodendrocyte precursors, distributed throughout the fetal WM, may be in particular concentrated within crossroad areas, thus contributing to their increased vulnerability. In other words, hypoxic-ischemic or inflammatory lesion during the period of maturation-dependent vulnerability of oligodendrocyte precursors may simultaneously have “diffuse” cytotoxic effects throughout the fetal WM as well as more prominent “focal” cytotoxic effects in periventricular crossroad areas.

In addition, the potential impact of the cytotoxic injury in crossroad areas is increased by the presence of other vulnerable populations of cells. For example, we demonstrated that an attenuated population of microglia characterizes some crossroad areas, as described by Baud et al (28), which can easily be activated in a cytotoxic cascade in the case of hypoxia-ischemia. Microglia is probably involved in removing axons and cells, which fail to reach their developmental target destination or to maintain their route along the signaling gradients during the normal development in nondamaged brains. This may explain our findings of microglial cells at several crossroads of callosal and projection fibers at the dorsal aspect of the frontal horn of the lateral ventricle in otherwise “normal” brains.

At present, there is no direct evidence on the nature of primary damage of the ECM, axonal guidance cue-producing cells, and axons in periventricular crossroad areas. It stands to reason, however, that these elements are almost certainly damaged, taking into the consideration massive disruptions and pathologic changes observed in the PVL and the PVH. Thus, our conjecture on the developmental importance of periventricular crossroad areas is in agreement with notions on the existence of both primary and secondary lesions after perinatal hypoxic-ischemic or inflammatory brain damage.

Conclusions

In comparison to lesions of more distal portions of the fetal WM, periventricular lesions frequently have a more adverse effect on the neurodevelopmental outcome. With respect to that, our study highlights several novel findings important for a proper interpretation of underlying pathogenetic-developmental events.

We advanced the conjecture that the proper interpretation of MR images of the immature brain as well as mechanisms leading to the differential neurodevelopmental outcome has to take into consideration the special arrangement of projection and associative fibers in the periventricular region as well as the fact that these fibers are embedded in the ECM enriched with axon guidance cues. To this end, we correlated MR imaging and histologic findings and identified different tissue components of the periventricular region. The major finding of our study is that in preterm infants before 33 POW, growing projection, commissural, and associative fibers form a complex grid embedded in the ECM rich in axonal guidance molecules; display characteristic histologic and MR imaging properties; and are located at typical predilection sites of the focal PVL.

With respect to the MR imaging analysis of the preterm infant’s cortex, the key fact is that periventricular crossroad areas may be wrongly interpreted as the PVL, because in MR images they present MR imaging signal intensity features similar to those in PVL (ie, they appear as localized periventricular areas of either decreased [on T1-weighted images] or increased [on T2-weighted images] MR imaging signal intensity). It is not surprising that lesions of these developmentally and topographically important periventricular crossroads of projection, commissural, and associative fibers usually have profound but variable effect on the subsequent development, organization, and function of motor, sensory, and cognitive neural pathways and systems.

On the basis of these developmental structural features, we have proposed that complex and multiple deficits caused by lesions of periventricular crossroad areas often extend beyond the limits of the developmental plasticity and may be difficult to compensate. Therefore, we also describe periventricular crossroad areas (and especially the main frontal crossroad area C1) as “crossroads of no return.” Finally, new data on

cellular events in periventricular crossroad areas may be useful for the refinement of MR imaging localization of lesion as well as for the development of better strategies of neuroprotection for the benefit of patients endangered by the preterm birth.

Acknowledgments

We thank Zdenka Cmuk, Danica Budinščak, and Božica Popović, for their excellent technical assistance.

References

- Volpe JJ. *Neurology of the newborn*. 4th ed. Philadelphia: WB Saunders;2001
- Volpe JJ. **Cerebral white matter injury of the premature infant: more common than you think.** *Pediatrics* 2003;112:176–180
- Johnston MV, Trescher WH, Ishida A, Nakajima W. **Neurobiology of hypoxic-ischemic injury in the developing brain.** *Pediatr Res* 2001;49:735–741
- Perlman JM. **White matter injury in the preterm infant: an important determination of abnormal neurodevelopment outcome.** *Early Hum Dev* 1998;53:99–120
- Rutherford MA, Pennock JM, Counsell SJ, et al. **Abnormal magnetic resonance signal in the internal capsule predicts poor neurodevelopmental outcome in infants with hypoxic-ischemic encephalopathy.** *Pediatrics* 1998;102:323–328
- De Vries LS, Groenendaal F, Van Haastert IC, et al. **Asymmetrical myelination of the posterior limb of the internal capsule in infants with periventricular haemorrhagic infarction: an early predictor of hemiplegia.** *Neuropediatrics* 1999;30:1–6
- Coskun A, Lequin M, Segal M, et al. **Quantitative analysis of MR images in asphyxiated neonates: correlation with neurodevelopmental outcome.** *AJNR Am J Neuroradiol* 2001;22:400–405
- Hoon AH Jr, Lawrie WT Jr, Melhem ER, et al. **Diffusion tensor imaging of periventricular leukomalacia shows affected sensory cortex white matter pathways.** *Neurology* 2002;59:752–756
- Banker BQ, Larroche JC. **Periventricular leukomalacia of infancy: a form of neonatal anoxic encephalopathy.** *Arch Neurol* 1962;7:386–410
- Leviton A, Gilles F. **Ventriculomegaly, delayed myelination, white matter hypoplasia, and “periventricular” leukomalacia: how are they related?** *Pediatr Neurol* 1996;15:127–136
- Moses P, Courchesne E, Stiles J, et al. **Regional size reduction in the human corpus callosum following pre- and perinatal brain injury.** *Cereb Cortex* 2000;10:1200–1210
- Okoshi Y, Itoh M, Takashima S. **Characteristic neuropathology and plasticity in periventricular leukomalacia.** *Pediatr Neurol* 2001;25:221–226
- Counsell SJ, Allsop JM, Harrison MC, et al. **Diffusion-weighted imaging of the brain in preterm infants with focal and diffuse white matter abnormality.** *Pediatrics* 2003;112:1–7
- Hüppi PS, Murphy B, Maier SE, et al. **Microstructural brain development after perinatal cerebral white matter injury assessed by diffusion tensor magnetic resonance imaging.** *Pediatrics* 2001;107:455–460
- Miller SP, Vigneron DB, Henry RG, et al. **Serial quantitative diffusion tensor MRI of the premature brain: development in newborns with and without injury.** *J Magn Reson Imaging* 2002;16:621–632
- Felderhoff-Mueser U, Rutherford MA, Squier WV, et al. **Relationship between MR imaging and histopathologic findings of the brain in extremely sick preterm infants.** *AJNR Am J Neuroradiol* 1999;20:1349–1357
- Childs AM, Ramenghi LA, Evans DJ, et al. **MR features of developing periventricular white matter in preterm infants: evidence of glial cell migration.** *AJNR Am J Neuroradiol* 1998;19:971–976
- Haynes RL, Folkner RD, Keefe RJ, et al. **Nitrosative and oxidative injury to premigrating oligodendrocytes in periventricular leukomalacia.** *J Neuropathol Exp Neurol* 2003;62:441–450
- Back SA. **Recent advances in human perinatal white matter injury.** *Progr Brain Res* 2001;132:131–147
- Govaert P, De Vries LS. *An atlas of neonatal brain sonography*. London: Mac Keith Press;1997
- von Monakow C. *Gehirmpathologie*. Vienna: Alfred Hölder;1905
- Yakovlev PI, Lecours AR. **The myelogenetic cycles of regional maturation of the brain.** In: Minkowski A, ed. *Regional development of the brain in early life*. Oxford: Blackwell;1967:3–70
- Meyer JW, Makris N, Bates JF, et al. **MRI-based topographic parcellation of human cerebral white matter.** *Neuroimage* 1999;9:1–17
- Kostović I, Judaš M, Radoš M, Hraba[caron]c P. **Laminar organization of the human fetal cerebrum revealed by histochemical markers and magnetic resonance imaging.** *Cereb Cortex* 2002;12:536–544
- Kostović I. **Structural and histochemical reorganization of the human prefrontal cortex during perinatal and postnatal life.** *Progr Brain Res* 1990;85:131–147
- Dammann O, Hagberg H, Leviton A. **Is periventricular leukomalacia an axonopathy as well as an oligopathy?** *Pediatr Res* 2001;49:453–457
- Evrard P. **Pathophysiology of perinatal brain damage.** *Dev Neurosci* 2001;23:171–174
- Baud O, Daire JL, Dalmaz Y, et al. **Gestational hypoxia induces white matter damage in neonatal rats: a new model of periventricular leukomalacia.** *Brain Pathol* 2004;14:1–10
- Kostović I, Goldman-Rakic PS. **Transient cholinesterase staining in the mediodorsal nucleus of the thalamus and its connections in the developing human and monkey brain.** *J Comp Neurol* 1983;219:431–447
- Gallyas F. **Silver staining of myelin by means of physical development.** *Neurol Res* 1979;1:203–209
- Hsu SM, Raine L, Fanger H. **The use of antiavidin antibody and avidin-biotin-peroxidase complex in immunoperoxidase techniques.** *Am J Clin Pathol* 1982;75:816–821
- Kostović I, Rakic P. **Developmental history of the transient subplate zone in the visual and somatosensory cortex of the macaque monkey and human brain.** *J Comp Neurol* 1990;297:441–470
- Brisse H, Fallet C, Sebag G, et al. **Supratentorial parenchyma in the developing fetal brain: in vitro MR study with histologic comparison.** *AJNR Am J Neuroradiol* 1997;18:1491–1497
- Girard NJ, Raybaud CA, Poncet M. **In vivo MR study of brain maturation in normal fetuses.** *AJNR Am J Neuroradiol* 1995;16:407–413
- Ulfing N, Chan WY. **Axonal patterns in the prosencephalon of the human developing brain.** *Neuroembryology* 2002;14:–16
- Honig LS, Herrmann K, Shatz CJ. **Developmental changes revealed by immunohistochemical markers in human cerebral cortex.** *Cereb Cortex* 1996;6:794–806
- His W. *Die Entwicklung des menschlichen Gehirns während der ersten Monate*. Leipzig: Hirzel;1904
- Maas LC, Mukherjee P, Carballido-Gamio J, et al. **Early laminar organization of the human cerebrum demonstrated with diffusion tensor imaging in extremely premature infants.** *Neuroimage* 2004;22:1134–1140
- Sbarbati A, Pizzini F, Fabene PF, et al. **Cerebral cortex three-dimensional profiling in human fetuses by magnetic resonance imaging.** *J Anat* 2004;204:465–474
- Kostović I, Judaš M. **Correlation between the sequential ingrowth of afferents and transient patterns of cortical lamination in preterm infants.** *Anat Rec* 2002;267:1–6
- Prayer D, Prayer L. **Diffusion-weighted magnetic resonance imaging of cerebral white matter development.** *Eur J Radiol* 2003;45(3): 235–243
- Smart IHM, Dehay C, Giroud P, et al. **Unique morphological features of the proliferative zones and postmitotic compartments of the neural epithelium giving rise to striate and extrastriate cortex in the monkey.** *Cereb Cortex* 2002;12:37–53
- Huisman TA, Martin E, Kubik-Huch R, Marincek B. **Fetal magnetic resonance imaging of the brain: technical considerations and normal brain development.** *Eur Radiol* 2002;12:1941–1951
- Kostović I, Judaš M, Rašin MR, et al. **Periventricular predilection sites of hypoxic-ischaemic injury in preterm infants contain crossroads of growing pathways embedded in extracellular matrix rich in molecular guidance cues.** 6th IBRO World Congress of Neuroscience. July 10–15, 2003, Prague, Czech Republic
- Chisholm A, Tessier-Lavigne M. **Conservation and divergence of axon guidance mechanisms.** *Curr Opin Neurobiol* 1999;9:603–615
- Judaš M, Jovanov-Milošević N, Rašin MR, et al. **Complex patterns and simple architects: molecular guidance cues for developing axonal pathways in the telencephalon.** In: Kostović I, ed. *Guidance cues in the developing brain*. Vol 32: *Progress in molecular and subcellular biology*. Berlin-Heidelberg: Springer-Verlag;2003:1–32

47. Pearlman AL, Sheppard AM. **Extracellular matrix in early cortical development.** *Progr Brain Res* 1996;108:119–134
48. Skalióra I, Adams R, Blakemore C. **Morphology and growth patterns of developing thalamocortical axons.** *J Neurosci* 2000;20:3650–3662
49. Rakic P, Ang SBC, Breunig J. **Setting the stage for cognition: genesis of the primate cerebral cortex.** In: *The cognitive neurosciences*, 3rd ed. MIT Press;2004;33–49
50. Letinic K, Zoncu R, Rakic P. **Origin of GABAergic neurons in the human neocortex.** *Nature* 2002;417:645–648
51. Marin O, Rubenstein JL. **A long, remarkable journey: tangential migration in the telencephalon.** *Nat Rev Neurosci* 2001;2:780–790